Video Article

A Model for Perineural Invasion in Head and Neck Squamous Cell Carcinoma

Phillip Huyett[1], Mark Gilbert[1], Lijun Liu[2], Robert L. Ferris[2], Seungwon Kim[1]

[1]Department of Otolaryngology, University of Pittsburgh Medical Center

[2]University of Pittsburgh Cancer Institute, Hillman Cancer Center

Correspondence to: Phillip Huyett at huyettpa@upmc.edu

URL: https://www.jove.com/video/55043
DOI: doi:10.3791/55043

Keywords: Cancer Research, Issue 119, head and neck cancer, squamous cell carcinoma, perineural invasion, dorsal root ganglion, matrigel, mouse model

Date Published: 1/5/2017

Citation: Huyett, P., Gilbert, M., Liu, L., Ferris, R.L., Kim, S. A Model for Perineural Invasion in Head and Neck Squamous Cell Carcinoma. *J. Vis. Exp.* (119), e55043, doi:10.3791/55043 (2017).

Abstract

Perineural invasion (PNI) is found in approximately 40% of head and neck squamous cell carcinomas (HNSCC). Despite multimodal treatment with surgery, radiation, and chemotherapy, locoregional recurrences and distant metastases occur at higher rates, and overall survival is decreased by 40% compared to HNSCC without PNI. *In vitro* studies of the pathways involved in HNSCC PNI have historically been challenging given the lack of a consistent, reproducible assay. Described here is the adaptation of the dorsal root ganglion (DRG) assay for the examination of PNI in HNSCC. In this model, DRG are harvested from the spinal column of a sacrificed nude mouse and placed within a semisolid matrix. Over the subsequent days, neurites are generated and grow in a radial pattern from the cell bodies of the DRG. HNSCC cell lines are then placed peripherally around the matrix and invade preferentially along the neurites toward the DRG. This method allows for rapid evaluation of multiple treatment conditions, with very high assay success rates and reproducibility.

Video Link

The video component of this article can be found at https://www.jove.com/video/55043/

Introduction

Head and neck squamous cell carcinoma (HNSCC) is the sixth most common cancer in the US, with 10,000 deaths per year nationally and 300,000 deaths per year worldwide[1]. The overall prognosis for HNSCC has remained unchanged at 50% for the past several decades. Perineural invasion (PNI) is one of the most prominent pathological features that portend a poor prognosis in patients with HNSCC. Unfortunately, PNI is a frequent occurrence in HNSCC and can be found in up to 40% of HNSCC patients[2,3].

PNI is the process by which malignant cells track along nerves to adjacent tissues, allowing for higher rates of local and distant spread. Accordingly, PNI-positive HNSCC tumors have higher rates of locoregional recurrences and distant metastases, resulting in lower overall survival compared to HNSCC patients without PNI[4-8].

Although the treatment of patients with PNI is typically maximized by employing surgery, radiation, and chemotherapy, the overall survival rates of these patients are still decreased by up to 40% compared to patients without PNI[9-11]. Thus, it is clear that the current treatment modalities for HNSCC are ineffective in improving the adverse prognosis associated with PNI. The approach of developing targeted therapy against PNI in HNSCC has been hindered by the poor understanding of the factors that regulate this process. This is, in part, a consequence of the lack of a consistent *in vitro* model for the study of PNI in HNSCC.

In recent years, several groups have been utilizing an *in vitro* model for studying PNI in predominantly pancreatic and prostate cancers[12-19]. This model uses the neurites generated from dorsal root ganglia isolated from mice or rats as a surrogate for large-nerve invasion. The dorsal root ganglia are fixed in a factor-depleted semisolid matrix, which is a solubilized basement membrane protein mixture secreted by Engelbreth-Holm-Swarm mouse sarcoma cells. This matrix allows for the outgrowth of the neurites and the tracking of single cancer cells along these neurites. Described here is the adaption of this model for the examination of PNI in HNSCC.

Protocol

1. Preparation of Culture Medium and Dishes (10 min)

1. Add 100 µL of Dulbecco's Modified Eagle Medium (DMEM) with 10% fetal bovine serum (FBS) to the wells of a 96-well V-bottom plate.
2. Remove a pre-aliquoted-vial of approximately 100 µL of semisolid matrix from the 20 °C freezer and place it directly on ice.

NOTE: Do this prior to the dorsal root ganglion (DRG) harvest because the semisolid matrix takes approximately 30 min to reach liquid state on ice, which is necessary for the subsequent steps. Failure to keep the semisolid matrix on ice at all times will result a poor-quality matrix droplet.

3. Label glass-bottom cultures plates with permanent ink, creating unique identifiers in each of the four corners on the undersurface of the plate. Place the plates right-side up on ice to cool the plate surface.
   NOTE: Each mouse yields 32 - 40 DRG, so label them from 1 to 40. It is not necessary to pre-chill pipet tips, as chilled tips will warm over the course of placing the matrix droplets, potentially introducing differences in matrix consistency.

2. Dissection of Murine DRG (45 min)

1. Euthanize an athymic nude mouse as per specific laboratory protocols, such as through the use of a CO_2 chamber and a thoracotomy.
2. Set up the dissection area and microscope. Use the clean, sterilized, and flat underside of polystyrene containers for 15- or 50-mL conical tubes.
   NOTE: Additionally, they are suitable for use as the dissecting surface, as they are inexpensive, disposable, and allow for fixation of the spine using pins or needles. Only use sterilized instruments and needles.
3. Under natural vision, make a longitudinal incision along the spinal column from the root of the tail to the head of the mouse with a pair of straight or curved fine scissors.
4. Use the same scissors to transversely divide below the sacral spine. Dissect both sides of the spine all the way up to the skull base using the scissors. At this point, ensure that the cervical spine is transected cranially as far as possible with scissors.
5. Observe the cervical end of the spinal column under the operating microscope at low power. The white spinal cord is apparent in the middle of a bony ring, which is surrounded by variable amounts of paraspinal muscles and soft tissue.
6. Split the dorsal or superior aspect of the first 2 - 3 vertebral bodies with microscopic spring scissors. Using the spring action of the scissors, open this initial bony cut to ensure that the vertebral body dissection occurred at the midline. Continue in small increments towards the sacral spine, and then bisect the spine by completing the identical cuts on the ventral or inferior aspect of the vertebral bodies.
   NOTE: Failure to ensure the midline dissection of the bony spinal column will result in a lower DRG yield.
7. At this point, the spinal column is divided into two halves. Place one hemi-spine aside, with the spinal cord in place and facing down on a sterile plate.
   NOTE: Leaving the spinal cord in place will prevent the DRGs from drying out, as the DRGs are deep to the spinal cord.
8. Secure either end of the other hemi-spine with two 18-gauge needles on the polystyrene dissecting platform. Starting at the cervical end (which is apparent because the spine is narrower, the DRG are closer to one another, and there are rib insertions), gently peel back the spinal cord from about 4 vertebral levels.
9. Observe the sensory nerves (usually two) connecting the DRG. In the area where the nerves insert to the DRG, gently grasp the surrounding fascia with microscopic forceps. Dissect and trim this fascia and other nerve tissue with the microscopic spring scissors to free up the DRG. Gentle retraction will bring the DRG out of its position within the bony spine.
   NOTE: Increasing the microscope power at this step is beneficial. Crush injury to the DRG will significantly limit the growth of neurites. This is avoided by never grasping the DRG directly, but rather by grasping the surrounding fascia.
10. Cut the peripheral nerve (the DRG generally has one peripheral nerve, which is deep relative to the dissecting view) with the microscopic spring scissors to release the DRG.
    NOTE: It is easiest to ascertain where the nerve ends and the DRG begins while on tension, so making this cut as close as possible to the DRG at this point is ideal. Once this distal branch is cut, the proximal branches are trimmed as well.
11. Trim the DRG of any stray nerve fibers or fascial attachments with the microscopic spring scissors. After adequate isolation, place the DRG into the room-temperature medium within the 96-well V-bottom plate.
    NOTE: Placing a dark background underneath the plate makes visualizing the sub-mm white DRGs easier. Only place one DRG in each well; this way, they can be accounted for more easily in the subsequent steps.
12. Repeat this process all the way down one hemi-spine and then the other. Each side yields 16 - 20 DRGs, totaling 32 - 40.
    NOTE: If there are fewer DRGs than this, the dissection of the spine needs to be carried out further cephalad and/or caudally. The DRGs become increasingly less well defined as one proceeds caudally.

3. Preparation of Semisolid Matrix Droplets (< 1 min per plate)

1. Remove one glass well-bottom plate from ice and place it on an ice block underneath the operating microscope. Make sure the aliquot of matrix remains on ice at all times.
2. Place a 1.5-µL droplet of matrix in each of the four corners of the glass-bottom plate with a 2-µL or 10-µL micropipetter, leaving a distance at least as great as the droplet itself from the edge of the glass well.
   1. Place the tip of the pipette directly onto the glass at a 45-degree angle. Slowly pipet the matrix. Slowly move away from the glass bottom after the matrix is engaged on the plate.
      NOTE: The surface tension between the matrix and glass should create a perfect hemisphere each time.
   2. Stop pipetting just before the tip is empty, because inadvertent injection of air into the matrix droplet makes the diameter of the matrix droplet far greater and is difficult to remove.
      NOTE: Using a second hand to stabilize the pipetting hand facilitates more accurate placement.

4. Insertion of DRG into Semisolid Matrix Droplets (< 2 min per plate)

1. Leave the plate with the matrix droplets briefly at room temperature (~ 1 min). This slightly stiffens the matrix, making it easier for the precise placement of the DRG.

2. Scoop (do not grasp) the DRG gently with closed microscopic forceps in the left hand. Again, a dark background against the small, white DRG facilitates visualization. Transfer the DRG to the tip of a 21-gauge needle in the right hand. This transfer will leave residual media on the forceps.
3. Gently insert the DRG into the middle of the matrix droplet using the 21-gauge needle (**Figure 1**). Most of the time, the DRG will easily release into the matrix and then can be positioned centrally with the needle.
    1. If the DRG sticks to the needle, use the microscopic forceps to push the DRG off of the needle and into the matrix droplet. Wick away excess media from the microscopic forceps with a lab wipe.
    NOTE: Introducing media to the matrix will alter the diameter, volume, and consistency of the assay. An ice block with color or colored writing provides background contrast, which eases visualization of this delicate process.
4. After the plate has all four DRGs, perform a final inspection to ensure that the DRG is in the center of the matrix droplet. Make adjustments as needed with the 21-guage needle.
5. Transfer the completed plate to a 37 °C incubator. This will solidify the semisolid matrix and fix the DRG in position.
6. Repeat this process for all of the DRGs. Place blank matrix droplets without a DRG as the negative control.
7. Add 4 mL of DMEM with 10% FBS media to each glass-bottom plate after completing all plates and exposing them to the 37 °C incubator for at least 3 min. Place the plate at a slight angle and slowly add the medium, such that it gradually comes into contact with the matrix-DRG units.
    NOTE: If the medium is added too quickly or vigorously, the matrix and/or DRG can become dislodged.
8. Store the assays in the 37 °C incubator for the next 48 - 72 h.
    NOTE: Periodic examination of the assays will show circumferential outgrowth of neurites towards the matrix edge (**Figure 2**). When the neurites are greater than three-fourths of the way to the matrix, it is appropriate to plate the cells.

5. Preparation of the Head and Neck Cancer Cells

NOTE: Cell lines other than head and neck squamous cell carcinoma cells can be used in this experimental design.

1. Maintain squamous cell carcinoma cell lines in DMEM with 10% FBS in preferred flasks or culture dishes in a 37 °C incubator. To prepare cells for experimentation, suction all the medium from the culture flask or dish and wash it twice with PBS. Suspend the cells by adding an appropriate amount of 0.025% trypsin for 5 min, followed by DMEM with 10% FBS. Pipette 4 mL of the cell and media mixture into 6-mL culture dishes.
    NOTE: A 6-mL culture plate provides more than enough cells, even when less than 50% confluent.
2. Expose the HNSCC cell lines to different conditions 24 h prior to staining and plating on the DRG assay. Re-dose the condition once the cells are plated to maintain a consistent environment.
    NOTE: Add antibodies, growth factors, cytokines, or other molecules to the cell culture dishes 1 - 2 days following mouse dissection and implantation of the DRG into the matrix.
3. Add fluorescent cell stains 1 h before plating the cells (2 - 3 days after the DRG harvest and implantation into the matrix).
    NOTE: The particular stains used here pass freely through the cell membrane; however, after reacting with intracellular thiol groups, the stain remains within the cell and is passed on to daughter cells. The staining greatly facilitates visualization within the assays. These temporary stains are ideal for these assays because the fluorescence is present for 2 - 3 days, which is the timeframe of these experiments. It also allows for the use of many different colors and obviates the need for creating fluorescent protein-transfected cell lines.
    1. Prepare 10 µM of dye solution by mixing 2 µL of 10 mM stock cell stains in 2 mL of serum-free DMEM for every cell condition. Warm this to 37 °C before adding it to cells.
    2. Remove the culture medium within the 6-mL plate, leaving the adherent HNSCC cells on the plate. Add 2 mL of phosphate-buffered saline (PBS) and remove 2 mL of the 10 µM cell stain/serum-free DMEM added to each plate
    3. Return the 6-mL culture plate with the cell stain to the 37 °C incubator for 40 min.
    4. After 40 min, aspirate the medium. Add 2 mL of PBS and then aspirate it. Add 1 mL of 0.025% trypsin to each plate and replace them in the 37 °C incubator.
    5. Add 2 mL of DMEM with 10% FBS after 3 - 5 min and transfer the suspended cells to a 15-mL conical tube. Spin the cells and re-suspended them in 1 mL of DMEM with 10% FBS.
    6. Count the cells with a hemocytometer or automated cell counter, and then add DMEM with 10% FBS to create a final cell concentration of 300,000 cells per mL.

6. Plating Head and Neck Cancer Cells

1. Remove the glass-bottom plates with the matrix-DRG assays from the incubator.
    NOTE: Again, they are appropriate when neurites are at least 75% of the way to the edge of the matrix, which generally occurs after 2 - 3 days. This is best seen using at least a 10X objective.
2. Aspirate the medium within the glass-bottom plate. Completely aspirate the medium within the glass well without removing the matrix-DRG units.
3. Draw up 200 µL of the 300,000 cells/mL medium using a 200-µL pipet. Place two drops of the cells over each matrix-DRG assay. Perform this step for each matrix droplet, creating four repeats of each cell condition on one plate.
    NOTE: The hemispherical shape of the matrix allows the cells to settle in a ring along the periphery of the assay (**Figure 3a, Figure 3b**). Finding a pipet with a smooth trigger makes placement of uniform drops far easier.
4. Confirm similar cell numbers and distribution of the various cell conditions under 4X microscopy.
5. Place the glass-bottom plates into the 37 °C incubator for approximately 60 min. NOTE: Although there is only a small volume of cells and media (~ 150 µL), the assays do not dry out until several hours of incubator time have elapsed.
6. After 60 min, gently add 4 mL of DMEM with 10% FBS along the sidewall of the glass-bottom plate.

NOTE: Over a period of time, the cells partially adhere to the plate bottom, and the method of adding the medium does not disturb the cells. Different cell types make take more or less time to begin to adhere to the glass-bottom plate.

7. Replace any exogenous drugs or growth factors at this time to maintain the previous concentration levels.
8. Return the assays to the 37 °C incubator, except when they are examined microscopically. Quantify the results of this assay by microscopic imaging. Briefly, count the strands of perineural invasion within four quadrants using a 4X microscopic image.
   NOTE: A microscope with a 4X objective and fluorescence capabilities is adequate for photo-documenting the assays. The size of the assays fits nicely within the field of a 4X objective, which is detailed enough to capture the individual areas of perineural invasion. Perineural invasion becomes apparent within 24 h, but beyond 48 h, the integrity of the assays begins to weaken, as the tumor cells divide along the periphery of the matrix and invade. Beyond 48 h, there is also substantial efflux of fibroblasts from the DRG, which obscures visualization using brightfield microscopy. Therefore, it is advisable to photo-document the results with 4X microscopy at least twice during this window (*e.g.,* at 24 and 48 h after plating the tumor cells). Be mindful that these are 3-dimensional assays, and it is difficult to completely image the entire assay. Most perineural invasion occurs in a plane from the bottom of the plate, where the cells are embedded in the matrix slightly above the bottom of the plate. Because this plane is close to horizontal, the vast majority of neurites with tumor cells are captured in a single-level image at 4X.

Representative Results

After the dissection of the DRG and the placement within the matrix droplet, the appearance of the assay should resemble **Figure 1.** Note that the DRG is not perfectly round, but it is centered within the matrix droplet. This allows for the outgrowth of neurites in 360 degrees, shown partially in **Figure 2**. Be aware that certain parts of the DRG send out neurites faster and in greater numbers than others, typically corresponding to where the efferent and afferent nerve branches entered and exited the DRG, respectively. We account for this and for size differences between DRGs by randomly plating the DRGs in groups of 4 and then randomly assigning a given plate to each cell condition.

As described above, we plate the HSNCC cell lines once the neurites have extended at least ¾ of the way to the edge of the matrix, which is typically on day 3. The added cells form a circumferential ring around the matrix (**Figure 3a**). We subsequently photograph the assays on day 4 (**Figure 3b**) and day 5 (**Figure 3c**). The cell line shown here (FaDu) demonstrates an above-average ability to track along neurites. The SQCCY1 cell line shown in **Figure 4**, however, shows little to no proclivity to invade the assays.

When using a new cell line, it is import to utilize several negative controls to examine how that particular cell line behaves around the assay. First, plate cells around a "blank" assay consisting of matrix alone (**Figure 5**). All cell lines that our lab has examined actively divide around the matrix but do not enter or extend over the top of the matrix. When excessive cells are left on top of the matrix, there can be significant growth over the matrix. This highlights the need to ensure that as many cells fall to the periphery of the matrix as possible, rather than being left to rest and divide on top of the matrix. This can be accomplished by gently tapping on the plates before the cells adhere or by pipetting small amounts of media directly on top of the matrix droplet once the cells have begun to adhere to the glass plate.

A second negative control, wherein the cells are plated on the same day that the DRG is placed within the matrix, can be run. The goal of this approach is to demonstrate that it is not a neurotropic attraction that drives the cells to the DRG, but rather that the presence of the neurites is mandatory. Furthermore, when tumor cells have resided along the periphery of the matrix for greater than 2 days, the matrix edge becomes indistinct. The matrix then begins to lift of off the glass bottom and can be found free-floating in the media shortly thereafter. For this reason, this protocol describes plating the HNSCC cells once the neurites have extended 75% of the distance to the edge of the matrix.

There are innumerable options for quantifying the results of what are visually very apparent differences between assays. In one such method, the images of the assays are divided into four quadrants with a vertical and a horizontal line (**Figure 6**). One point is assigned for every quadrant that has at least one string of PNI. If the PNI extends beyond 50% of the way from the edge of the matrix to the DRG, then 2 points are assigned instead. In this way, a score of 0 - 8 points can be assigned. The major advantage to this system is that assays that have too many PNI units to count can be rapidly assessed. A disadvantage is that is does not adequately express the degree of PNI (*i.e.,* a quadrant with 1 neurite with invasion 100% of the distance to the DRG receives the same score (2) as a quadrant with 10 similarly-invaded neurites). Comparison of the brightfield and fluorescent images makes this system very easy, even with significant fibroblast efflux.

Sample scoring is shown in **Figure 6**. Using this four-quadrant scoring system for **Figure 3**, 0 points, 2 points, and 7 points were assigned for panels **Figure 3a**, **Figure 3a**, and **Figure 3c**, respectively. **Figure 4** received a score of 2 points and 2 points in panels **Figure 4a** and **Figure 4b**, respectively. The data in **Table 1** depicts the results of several experiments using the cell lines FaDu and SQCCY1. Note that even with a limited grading scale such as this, statistically-significant differences in the mean four-quadrant scores are readily obtained using the independent samples t-test.

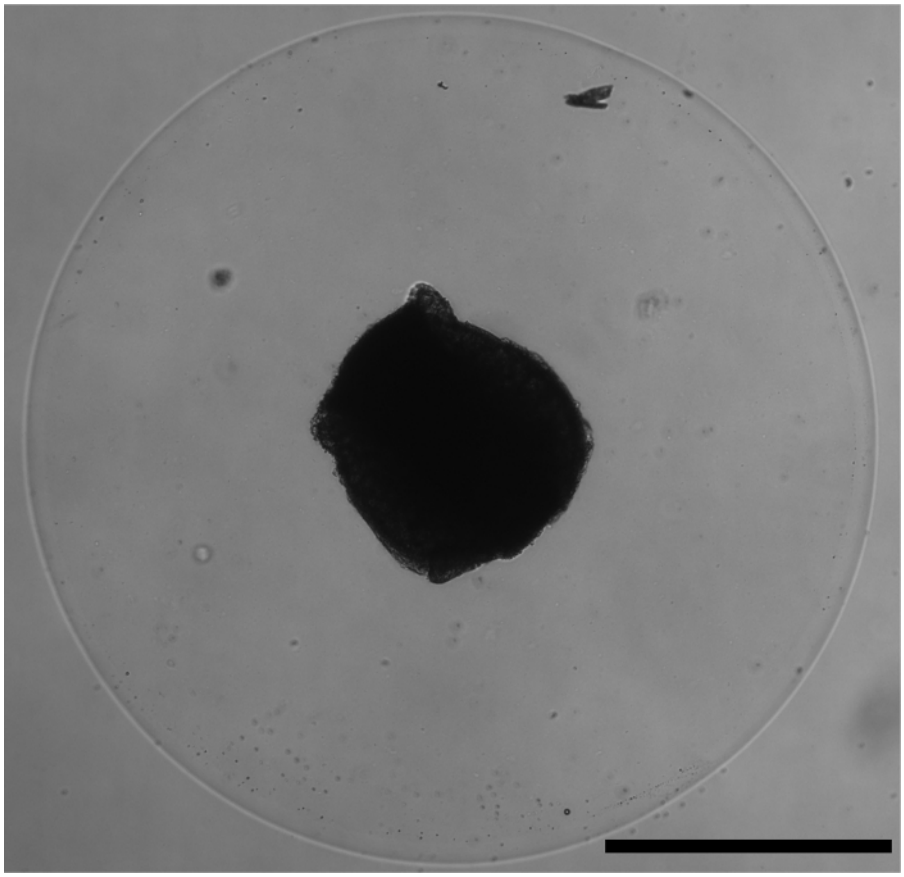

Figure 1. DRG-matrix Assay. Correct placement of the dorsal root ganglion within the matrix droplet, shown with brightfield microscopy at 4X. Scale bar represents 1 mm. Please click here to view a larger version of this figure.

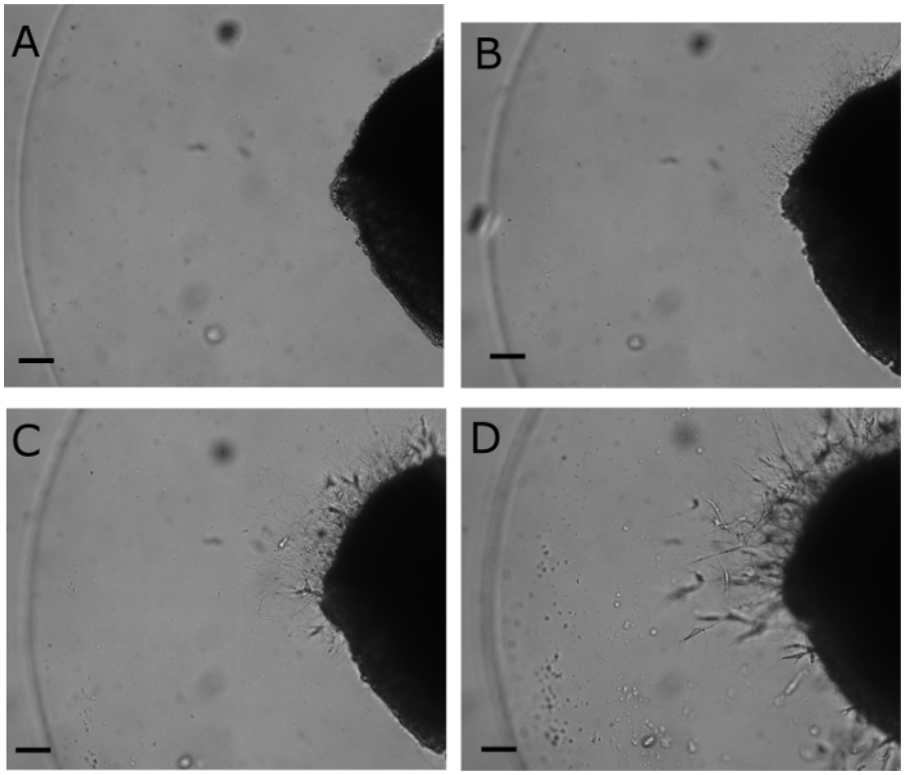

Figure 2. Outgrowth of Neurites. Neurites are absent on day 0 immediately after placing the DRG in the matrix droplet **(A).** By day 1 **(B)**, neurite outgrowth is apparent at 10X on brightfield microscopy. Neurite growth continues on day 2 **(C)** and day 3 **(D)**; however, note the efflux of the fibroblasts. Scale bar represents 0.1 mm. Please click here to view a larger version of this figure.

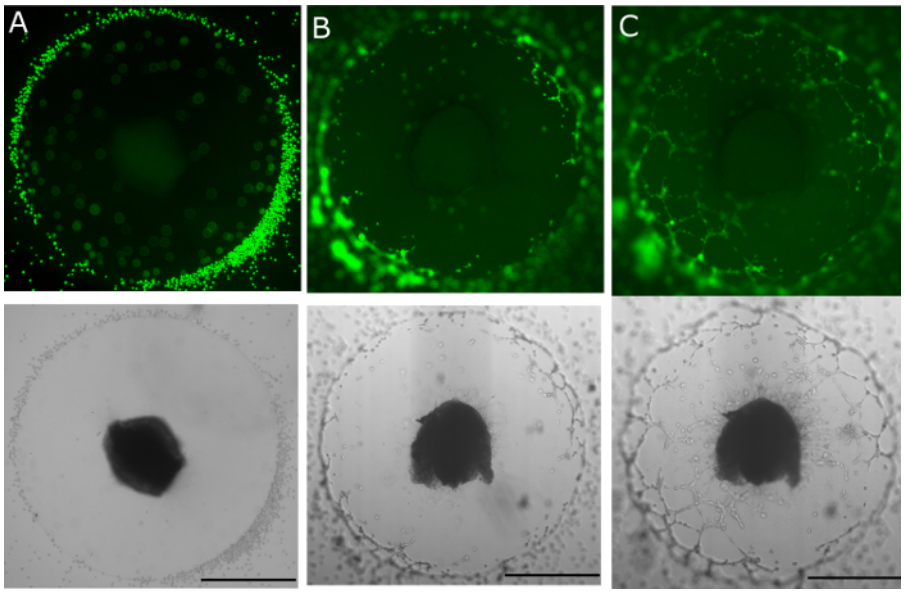

Figure 3. DRG-matrix Assay with FaDu. Head and neck squamous cell carcinoma line FaDu added peripherally around an assay on day 3 **(A)**, shown in green fluorescent and brightfield microscopy at 4X Progressive neural invasion is seen on day 4 **(B)** and day 5 **(C)**. Scale bar represents 1 mm. Please click here to view a larger version of this figure.

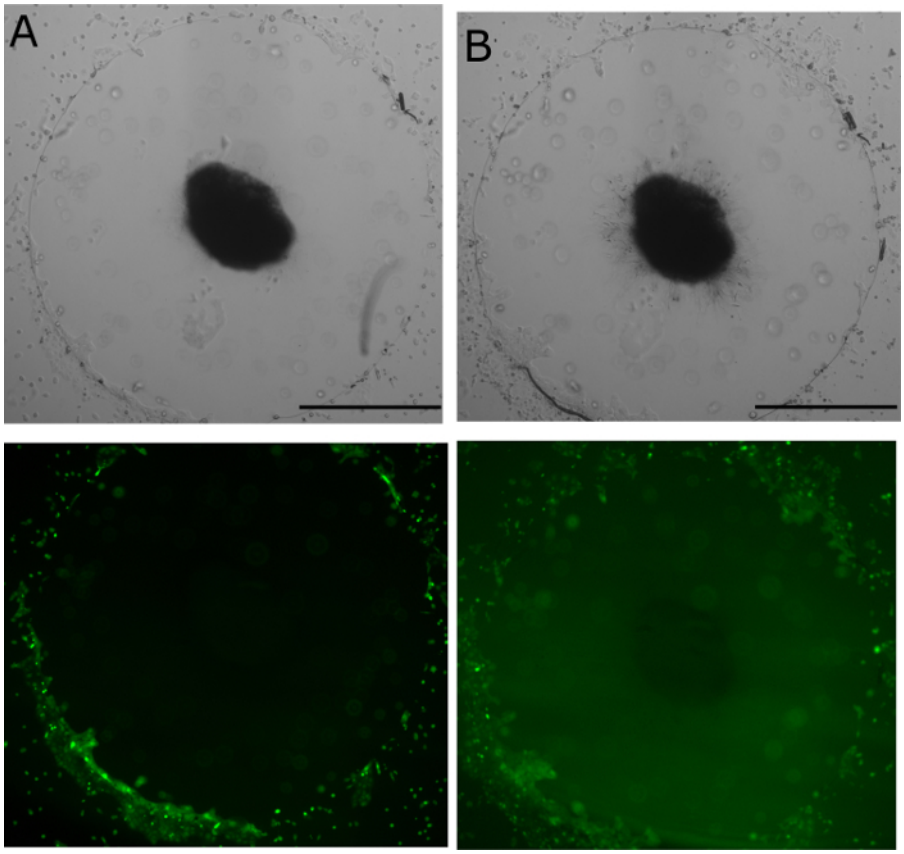

Figure 4. DRG-matrix Assay with SQCCY1. Head and neck squamous cell line SQCCY1 added on day 4 **(A)**, shown in brightfield and green fluorescent microscopy at 4X. Note that this cell line is not as proficient at perineural invasion as FaDu, even by day 5 **(B)**. Scale bar represents 1 mm. Please click here to view a larger version of this figure.

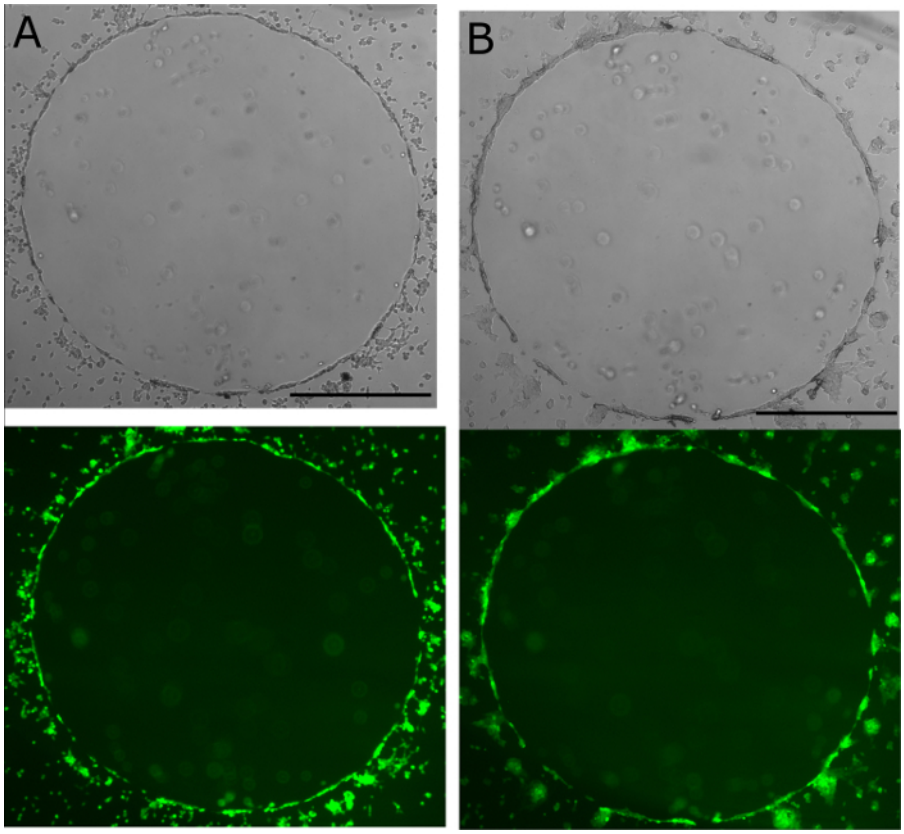

Figure 5. Matrix Assay with FaDu. Head and neck squamous cell carcinoma cell line FaDu added around a matrix droplet without a DRG on day 3. brightfield and green fluorescent microscopy (4X) shown on day 4 **(A)**. Note that the tumor cells do not enter the matrix or grow over the top of it, even by day 5 **(B)**. Scale bar represents 1 mm. Please click here to view a larger version of this figure.

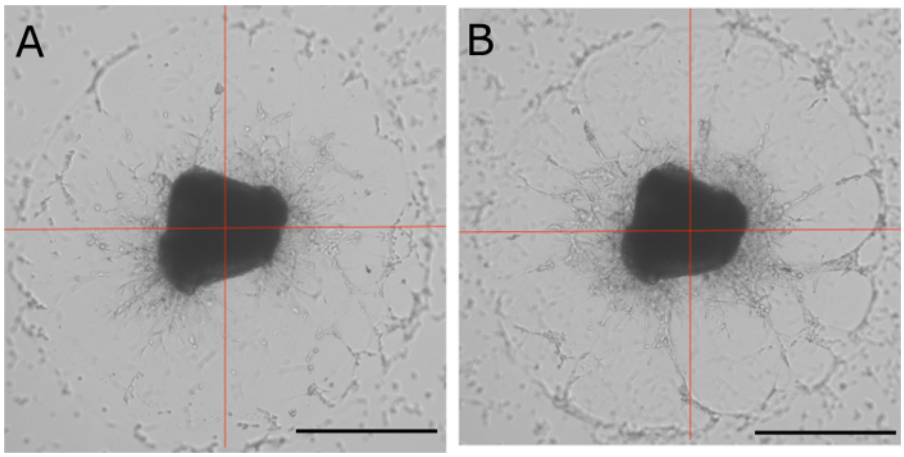

Figure 6. Four-quadrant Method for Assay Quantification. One point is assigned for every quadrant with a PNI less than 50% of the distance from the edge of the matrix to the DRG. 2 points are assigned when the PNI extends beyond 50%. The first example **(A)** would receive a score of 5 (1 point for every quadrant for a PNI less than 50%, except the bottom right, which has a PNI extending beyond 50%, where 2 points are scored). The second example **(B)** is scored as an 8 (a PNI beyond 50% in all four quadrants). Scale bar represents 1 mm. Please click here to view a larger version of this figure.

Cell line	n	Day 4	SD	P-value	Day 5	SD	P-value
FaDu	24	2.88	1.42	Ref	6.04	0.35	Ref
SQCCY1	20	0.60	0.60	<0.001	1.05	0.17	<0.001

Table 1. Comparison of the PNI Between FaDu and SQCCY1. Mean four-quadrant scores as shown in **Figure 6** between the cell lines FaDu and SQCCY1 at 24 h (day 4) and 48 h (day 5) after the cells were plated around the DRG-matrix assay. Comparisons are made using the independent sample t-test and presented with the standard deviation (SD) and P-values.

Discussion

Critical Steps within the Protocol

The most important steps within this protocol are the precise dissection and extraction of the dorsal root ganglia. Proper transection of the spinal column and a midline-longitudinal division into two hemi-spines are critical to obtaining large numbers of DRG. During the dissection of individual DRGs, the ganglion should never be handled directly, but rather the surrounding fascia should be grasped with the microscopic forceps. Failure to do this will result in a crush injury of the DRG, which is likely the major cause of failure for neurite outgrowth. It is far better to under-trim the surrounding neural tissues during dissection than to risk over-handling the DRG and obtaining no neurite growth in the assay.

Modifications and Troubleshooting

The experimental protocol as described above reflects the optimal methodology established from a large number of procedural adjustments made over several years. Listed directly under the corresponding step in the protocol section is a number of notes and pitfalls that resulted from the experiences of the authors when using this methodology. Given the number of steps involved, there are indeed many modifications that can be made to this protocol by future investigators. As experience with these modifications grows, it is anticipated that additional means of troubleshooting will be developed according to the preferences of the investigating team.

Limitations of the Technique

There are three major limitations to this technique. The first is that very fine neurites are used as a surrogate for large neural invasion, which is what pathologists observe in tumor specimens. It is not known what the role of neurites, as opposed to neurons, are *in vivo* because identifying perineurite invasion is beyond the capabilities of a routine histopathological exam. Secondly, perineural invasion is a form of soft-tissue invasion that may not simply involve tumor cells and an adjacent neuron, as is simulated in this assay. As such, exogenous factors native to the *in vitro* tumor milieu are lacking in this assay. Finally, the time period during which PNI can be studied is limited to approximately 48 h due to the combination of fibroblast efflux and loss of matrix integrity. In this way, cell lines that are effective at neural invasion but are slow dividing and/or invading will be missed and presumed to not be proficient at PNI.

Significance of the Technique with Respect to Existing/Alternative Methods

To our knowledge, this is the only *in vitro* model currently available to examine PNI in HNSCC. Given the frequency with which PNI occurs in HNSCC and the limited knowledge of mechanisms that currently exists, this method is advantageous for several reasons. First, it has a very high success rate and excellent reproducibility. The total experiment time is also relatively short compared to similar protocols[12,17-19]. Finally, with the large number of assays that can be generated from a single mouse, many conditions can be tested with scientifically-appropriate replicates. The combination of these factors allows for the rapid assessment of many different conditions with consistent results.

At the same time, the high quality of the assay permits more detailed examination of the interaction between the tumor cells and the neurites. The use of live-cell imaging allows for the appreciation of the neurite outgrowth process and the HSNCC cell invasion in time-lapse video form. The addition of fluorescently-stained cells creates very clear differentiation between the cancer cells and background material, such as fibroblasts and dense neurite outgrowth (which auto-fluoresce red). Whether following this protocol or those described by others, this general experimental design is in its relative infancy, and there is far from a gold standard for the *in vitro* study of PNI. For these reasons, the more approaches to this assay that are described in detail, the greater the opportunity for the collaborative development of an ideal methodology.

Future Applications or Directions after Mastering This Technique

Just as there are several different approaches to setting up the assays, there are several approaches to measuring the results. In the above text, a single method for rapidly quantifying the degree of perineural invasion in each assay was presented. This is ideal for screening the impact of numerous different pathways on PNI, especially given that one can isolate 32 - 40 DRGs per mouse. There are a number of advanced imaging techniques to assess PNI, including the amount of fluorescence within a given area, the distance and rate of cell invasion, and the raw number of cells within the assay. Once the dynamic portion of the experiment is finished, the cells within the assay and/or the supernatant can also be collected for further molecular analysis.

This experimental methodology offers the opportunity to elucidate mechanisms involved in the PNI of HNSCC and other cancers. This knowledge can drive the development of therapeutics to target the pathways of PNI, which, at the present time, are lacking in HNSCC. Specific targeting of PNI when identified as an adverse pathological feature can potentially obviate the need for the non-specific adjuvant treatments, such as radiation therapy and chemotherapy, that are currently utilized.

Disclosures

The authors have no competing financial interests.

Acknowledgements

This work was supported in whole by funding from the NIH through the R21 grant, "Mechanisms of Perineural Invasion in Head and Neck Cancer" and the NCI T32 training grant, "Post-Doctoral Research Training in Head and Neck Oncology (2T32CA060397-21)." Thank you to Richard Steiman, MD, PhD and lab staff.

References

1. Jemal, A. *et al.* Cancer statistics, 2006. *CA Cancer J Clin.* **56** (2), 106-130 (2006).
2. Hinerman, R. W. *et al.* Postoperative irradiation for squamous cell carcinoma of the oral cavity: 35-year experience. *Head Neck.* **26** (11), 984-994 (2004).
3. Rahima, B., Shingaki, S., Nagata, M., & Saito, C. Prognostic significance of perineural invasion in oral and oropharyngeal carcinoma. *Oral Surg Oral Med Oral Pathol Oral Radiol Endod.* **97** (4), 423-431 (2004).
4. Woolgar, J. A., & Scott, J. Prediction of cervical lymph node metastasis in squamous cell carcinoma of the tongue/floor of mouth. *Head Neck.* **17** (6), 463-472 (1995).
5. Tai, S. K. *et al.* Treatment for T1-2 oral squamous cell carcinoma with or without perineural invasion: neck dissection and postoperative adjuvant therapy. *Ann Surg Oncol.* **19** (6), 1995-2002 (2012).
6. George, D. L. *et al.* Nosocomial sinusitis in patients in the medical intensive care unit: a prospective epidemiological study. *Clin Infect Dis.* **27** (3), 463-470 (1998).
7. Fagan, J. J. *et al.* Perineural invasion in squamous cell carcinoma of the head and neck. *Arch Otolaryngol Head Neck Surg.* **124** (6), 637-640 (1998).
8. Soo, K. C. *et al.* Prognostic implications of perineural spread in squamous carcinomas of the head and neck. *Laryngoscope.* **96** (10), 1145-1148 (1986).
9. Parsons, J. T., Mendenhall, W. M., Stringer, S. P., Cassisi, N. J., & Million, R. R. An analysis of factors influencing the outcome of postoperative irradiation for squamous cell carcinoma of the oral cavity. *Int J Radiat Oncol Biol Phys.* **39** (1), 137-148 (1997).
10. Liao, C. T. *et al.* Does adjuvant radiation therapy improve outcomes in pT1-3N0 oral cavity cancer with tumor-free margins and perineural invasion? *Int J Radiat Oncol Biol Phys.* **71** (2), 371-376 (2008).
11. Fan, K. H. *et al.* Treatment results of postoperative radiotherapy on squamous cell carcinoma of the oral cavity: coexistence of multiple minor risk factors results in higher recurrence rates. *Int J Radiat Oncol Biol Phys.* **77** (4), 1024-1029 (2010).
12. Dai, H. *et al.* Enhanced survival in perineural invasion of pancreatic cancer: an in vitro approach. *Hum Pathol.* **38** (2), 299-307 (2007).
13. Ceyhan, G. O. *et al.* Neural invasion in pancreatic cancer: a mutual tropism between neurons and cancer cells. *Biochem Biophys Res Commun.* **374** (3), 442-447 (2008).
14. Gil, Z. *et al.* Paracrine regulation of pancreatic cancer cell invasion by peripheral nerves. *J Natl Cancer Inst.* **102** (2), 107-118 (2010).
15. He, S. *et al.* GFRalpha1 released by nerves enhances cancer cell perineural invasion through GDNF-RET signaling. *Proc Natl Acad Sci U S A.* **111** (19), E2008-2017 (2014).
16. He, S. *et al.* The chemokine (CCL2-CCR2) signaling axis mediates perineural invasion. *Mol Cancer Res.* **13** (2), 380-390 (2015).
17. Bakst, R. L. *et al.* Radiation impairs perineural invasion by modulating the nerve microenvironment. *PLoS One.* **7** (6), e39925 (2012).
18. Ayala, G. E. *et al.* In vitro dorsal root ganglia and human prostate cell line interaction: redefining perineural invasion in prostate cancer. *Prostate.* **49** (3), 213-223 (2001).
19. Na'ara, S., Gil, Z., & Amit, M. In Vitro Modeling of Cancerous Neural Invasion: The Dorsal Root Ganglion Model. *J Vis Exp.* (110) (2016).

